

Spontaneous opinion swings in the voter model with latency

Giovanni Palermo ^{1,2,*}, Anna Mancini ^{3,2}, Antonio Desiderio ^{3,2}, Riccardo Di Clemente,⁴ and Giulio Cimini^{3,2}

¹*Physics Department, Sapienza University of Rome, 00185 Rome, Italy*

²*Enrico Fermi Research Center, 00184 Rome, Italy*

³*Physics Department and INFN, University of Rome Tor Vergata, 00133 Rome, Italy*

⁴*Network Science Institute, Northeastern University London, London E1W1LP, United Kingdom*



(Received 31 January 2024; accepted 28 June 2024; published 26 August 2024)

The cognitive process of opinion formation is often characterized by stubbornness or resistance of agents to changes of opinion. To capture this feature we introduce a constant latency time in the standard voter model of opinion dynamics: after switching opinion, an agent must keep it for a while. This seemingly simple modification drastically changes the stochastic diffusive behavior of the original model, leading to deterministic dynamical oscillations in the average opinion of the agents. We explain the origin of the oscillations and develop a mathematical formulation of the dynamics that is confirmed by extensive numerical simulations. We further characterize the rich phase space of the model and its asymptotic behavior. Our work offers insights into understanding and modeling the phenomenon of *opinion swings*, often observed in diverse social contexts.

DOI: [10.1103/PhysRevE.110.024313](https://doi.org/10.1103/PhysRevE.110.024313)

I. INTRODUCTION

Binary-choice opinion formation models are popular in the statistical physics community for describing the evolution of opinions within a population of interacting agents [1–4]. As for spin systems, in these models the opinion of an agent can take one of two possible values and is influenced by the opinions of other agents through simple dynamic rules, which are iterated until a stable state (ordered or disordered) is reached—either consensus or coexistence of different opinions. The *voter model* [5,6] is a paradigmatic framework where an agent changes opinion by copying a randomly chosen neighbor, thus mimicking the processes of conformation and peer influence on the individual’s mind [7,8]. The model has been studied extensively and has found applications in many fields. Moreover, it is one of the very few nonequilibrium stochastic processes that can be solved exactly in any dimension [9].

Models of opinion dynamics provide useful tools to probe sociopolitical scenarios, test descriptive theories of collective behavior for consistency, and explore emergent phenomena [10]. However, they are based on simplified hypotheses of human interaction that neglect a lot of psychological and social factors influencing the decisions of individuals. Thus a lot of effort has been put into extending the basic models by incorporating more realistic aspects of opinion making [3,4], as well as calibrating model features on empirical data [11]. Some models try to incorporate a sort of reluctance of the agents to change opinion [12], often observed in empirical studies [13,14]. The extreme example in this direction is the voter model with “zealots” [3,15], where the presence of stubborn agents who do not change opinion at all determines

the route to the consensus state [16,17]. Other approaches consider memory-dependent rules for opinion changes. In the model by Stark *et al.* [18], changes of opinions are subject to inertia (the longer an agent maintains her opinion, the less likely she will change it), which can speed up or slow down the reaching of consensus. A similar behavior is observed in the model by Wang *et al.* [19], characterized by a freezing period (agents who changed opinions are less likely to change it in the short run). In the model with “aging” by Pérez *et al.* [20] (and subsequent developments [21,22]), opinions are more or less likely to change depending on how long they are held by agents. When agents prefer to adopt the older opinions, consensus is quickly reached, whereas a coexistence of states is possible if they prefer the more recent opinions. A simple mechanism for representing a cost or restriction associated with changing opinion was first proposed in the “latent” voter model by Lambiotte *et al.* [23]: after changing opinion, an agent sticks to it for a stochastic latency period. This additional rule drives the system away from the consensus state, as the two opinions coexist in the system for very long times. The latent voter model has been further studied in the limit of small, exponentially distributed latency times [24] and, for slightly different dynamical rules, in the context of differential latencies for the two opinions [25,26].

Concerning model validation, election data represent an ideal test ground to identify which mechanisms are the most relevant in emulating the opinion dynamics of humans [28–30]. A handful of studies managed to reproduce some statistical regularities of how votes in US presidential elections (a natural binary opinion setup) are distributed in the population. Fernández-Gracia *et al.* [28] were able to capture vote-share fluctuations across counties and long-range spatial correlations using a noisy voter model with the addition of recurrent mobility of agents. Braha and de Aguiar [29] extended the voter model with opinion leaders and external influence,

*Contact author: giovanni.palermo@cref.it

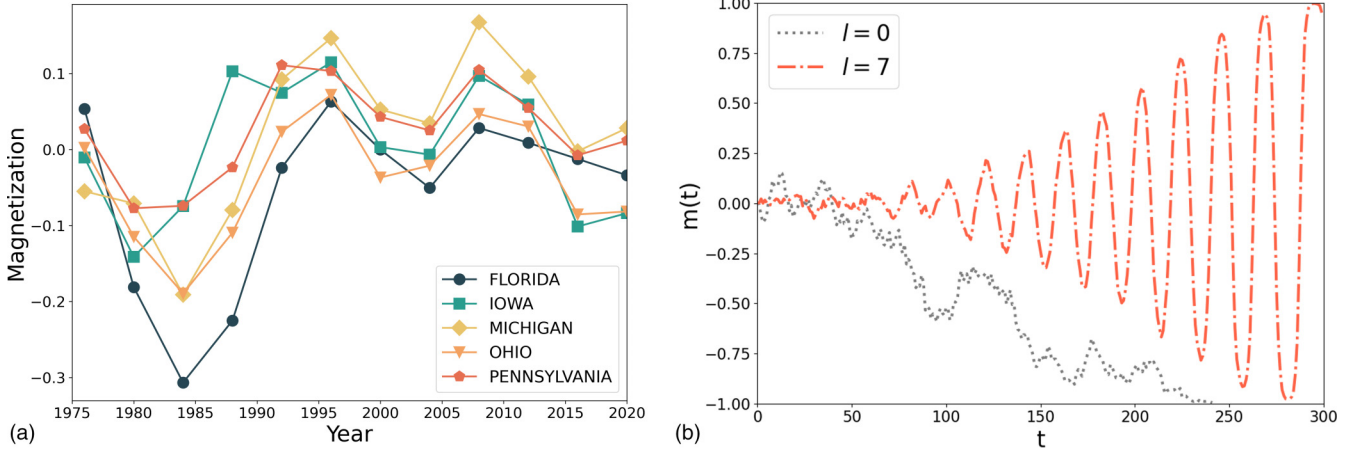


FIG. 1. (a) Results of U.S. presidential elections in a sample of *swing states* [27] (we assign +1 to votes for Democrats and -1 for Republicans; third parties are discarded, as they account for less than 10% of the votes). The dynamic exhibits oscillatory patterns, with similar periods set by the recurrence of elections every four years. (b) Evolution of the magnetization $m(t)$ in a single run of VM and VML, for a population of $N = 1000$ agents (the VM can be recovered as a special case of the VML by setting a latency time $l = 0$).

reproducing geographical patterns of vote-share distribution and social influence. A recurring feature observed in electoral data is the presence of opinion waves, especially for the so-called *swing states* [31], whose temporal patterns are determined by the regular occurrence of elections [see Fig. 1(a) and Appendix A]. The presence of seemingly regular oscillations of opinions is widely observed not only for political cycles [32,33] but also for census data on “partisan” issues [34], such as being pro or against the death penalty or tax increase, for trend reversals in fashion, economic cycles [35], and many more contexts.

In this work we report the emergence of regular opinion swings in binary models of opinion formation. We do so using the framework of the latent voter model, introducing a homogeneous latency time for each agent after a change of opinion. The assumption of the latency time is realistic for partisan issues or in political elections, where a voter switching party will hardly rethink her decision soon [23]. Additionally, in these situations a natural timescale exists (the regular occurrence of elections) and sets the same latency time for each agent. The introduction of a homogeneous latency time in the voter model leads to the emergence of oscillations in the average opinion which are not a consequence of stochastic fluctuations but arise from a deterministic drift due to the non-Markovianity of the update rule.

We explain the reason behind the occurrence of such opinion waves and provide a mathematical description of the model in the mean-field regime. Through extensive numerical simulations, we characterize the rich phase space of the model, featuring a transition from a constantly swinging opinion to full consensus for finite systems, whereas, in the thermodynamic limit, opinions keep swinging forever.

II. VOTER MODEL WITH LATENCY

We consider a population of N agents, located on the nodes of a fully connected graph. Each agent i is assigned with a spin taking values $s_i \in \{\pm 1\}$, representing her binary-state opinion. At each time step of the dynamics, each agent changes opinion

by adopting that of a randomly chosen neighbor. With respect to the standard voter model, here we introduce a constant *latency time* l : when an agent changes opinion she becomes inactive and cannot change it further for the subsequent l time steps (however, she can still influence others).¹ We remind the reader to Appendix B for full details on the simulations.

The voter model with latency (VML) thus formulated has a completely different behavior than the original voter dynamics [see Fig. 1(b)]. In the latter the average opinion of the population, given by the magnetization $m = \frac{1}{N} \sum_{i=1}^N s_i$, follows a stochastic evolution leading to consensus in a time that scales as \sqrt{N} . The VML is instead characterized by a predictable evolution in which $m(t)$ oscillates with a specific frequency and an amplitude that quickly approaches a value close to 1.² As we will see, such oscillations can eventually reach the consensus state $|m| = 1$ as a finite-size effect.

A. Model dynamics

We denote by $N_+(t)$ and $N_-(t)$ the number of agents with spin-up and -down, respectively, while $L_+(t)$ and $L_-(t)$ are the agents with spin-up and -down who are in the latency state. To characterize the evolution of the system, besides the magnetization $m(t) = [N_+(t) - N_-(t)]/N$ we use the fraction of agents in the latent state with positive and negative spin, respectively $\lambda_+(t) = L_+(t)/N$ and $\lambda_-(t) = L_-(t)/N$. Thus $\lambda(t) = \lambda_+(t) + \lambda_-(t)$ is the total fraction of agents in the latent state. Unless differently stated, we consider initial

¹Such a modification was originally introduced by Lambiotte *et al.* [23], yet in a different fashion, as an agent in the latent state is reactivated with a fixed probability at each step. Here instead, the agent exits the latent state after a fixed number of time steps.

²This behavior is also totally different from what is observed in [23], where the stochastic latency leads to a diffusive dynamics that remains at around $m = 0$.

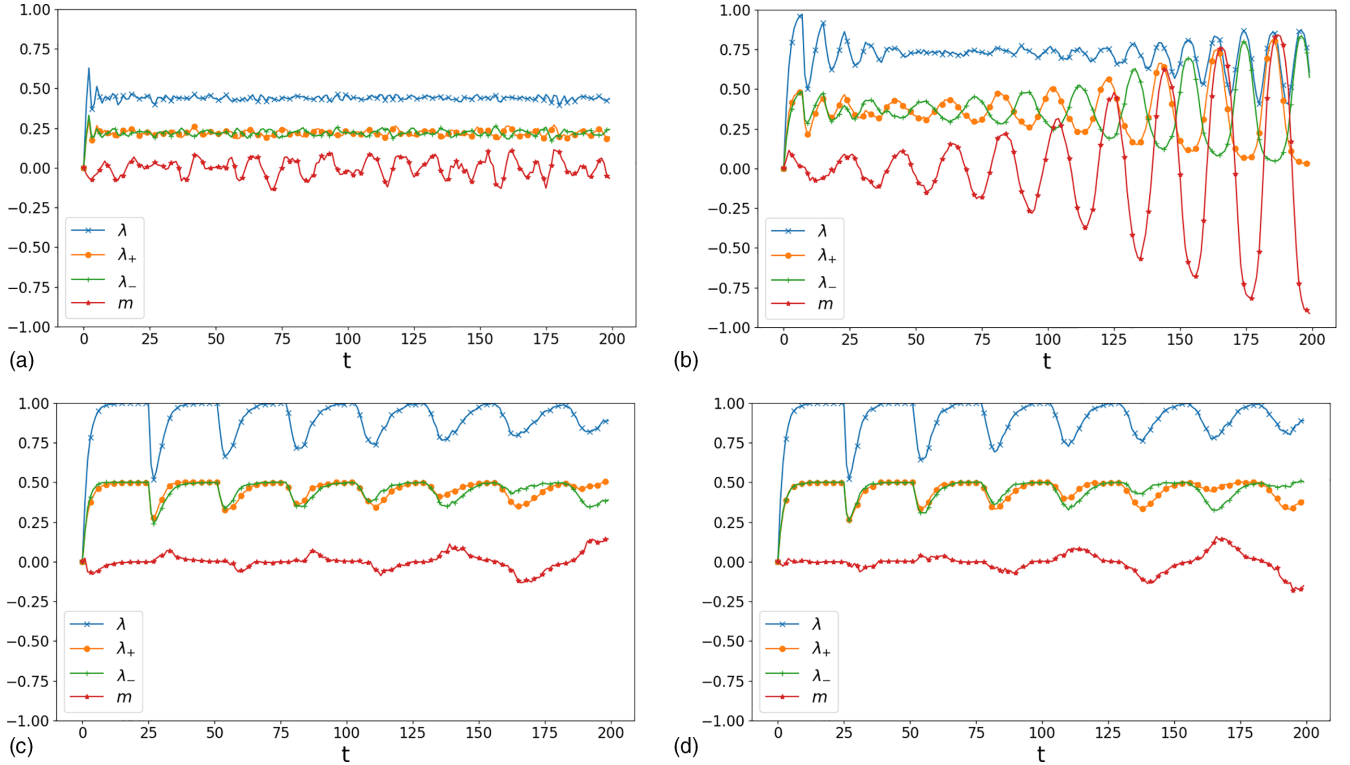


FIG. 2. Evolution of model variables with $l = 2$ (a), $l = 7$ (b), $l = 15$ (c) and $l = 25$ (d), for a population of $N = 1000$ agents. Short latency times (a) keep the system in a noisy state around $m = 0$, while high values of latency (d) freeze the agents for too long, altering the nature of the oscillations. In the intermediate regime (b) and (c), a clear oscillatory pattern quickly arises from noise.

conditions of zero magnetization, $m(0) = 0$, and no agent in the latency state, $\lambda(0) = 0$.³

Figure 2 provides sample realizations of the system for different values of latency l . For small values of l [Fig. 2(a)], oscillations have a small amplitude and are characterized by a certain level of randomness. For longer latency l , oscillations become extremely regular and with an amplitude close to 1 [Figs. 2(b) and 2(c)], whereas for even larger values the oscillatory pattern emerges after a long transient [Fig. 2(d)].

To analytically characterize the model, we start by writing down the equations for the time evolution of such quantities in the mean-field regime. We set the timescale so that we have N opinion updates in each time step of the dynamics (one for each agent). Denote by $\phi_{-+}(t)$ the probability of a spin-flip (i.e., that an agent changes her opinion) from -1 to $+1$ at time t , and by $\phi_{+-}(t)$ the probability of the opposite flip. The expected value of $\lambda(t)$ is thus given by the sum of all the flip probabilities in the past l steps:

$$E[\lambda(t)] = \sum_{\tau=0}^l [\phi_{-+}(t-\tau) + \phi_{+-}(t-\tau)], \quad (1)$$

³Opinion swings persist when we put some agents in the latent state at the beginning of the simulation. Likewise, the role of the initial magnetization is marginal, as the initial configuration is quickly forgotten by the dynamics.

where the two terms correspond to the expected values of $\lambda_{+}(t)$ and $\lambda_{-}(t)$:

$$E[\lambda_{\pm}(t)] = \sum_{\tau=0}^l \phi_{\mp\pm}(t-\tau). \quad (2)$$

In these equations, we only sum all flips that occurred in the last l steps, since agents exit from latency afterwards. On the contrary, to compute the magnetization we need to account for all the flips that occurred in the evolution of the system up to time t :⁴

$$E[m(t)] = 2 \sum_{\tau=1}^t [\phi_{-+}(\tau) - \phi_{+-}(\tau)]. \quad (3)$$

We now drop the notation $E[\dots]$ and switch from discrete to continuous time. We can connect the equations by showing how the spin-flip probabilities depend on these variables. To compute $\phi_{\mp\pm}$ we have to consider the probabilities of three occurrences: pick an agent who is not in the latency state; the selected agent has spin ∓ 1 ; pick a neighbor (i.e., a generic

⁴To derive this equation we start from the evolution of an individual spin in a single time step: $s_i(t) = s_i(t-1) + 2[\phi_{-+}(t) - \phi_{+-}(t)]$. Iterating the above expression we get $s_i(t) = s_i(t-t') + 2 \sum_{\tau=t-t'+1}^t [\phi_{-+}(\tau) - \phi_{+-}(\tau)]$, which in the limit $t' \rightarrow t$ leads to $s_i(t) = s_i(0) + 2 \sum_{\tau=1}^t [\phi_{-+}(\tau) - \phi_{+-}(\tau)]$. Averaging over all N spins, considering that $m(0) = 0$ and that we make N updates at each step, we get to Eq. (3).

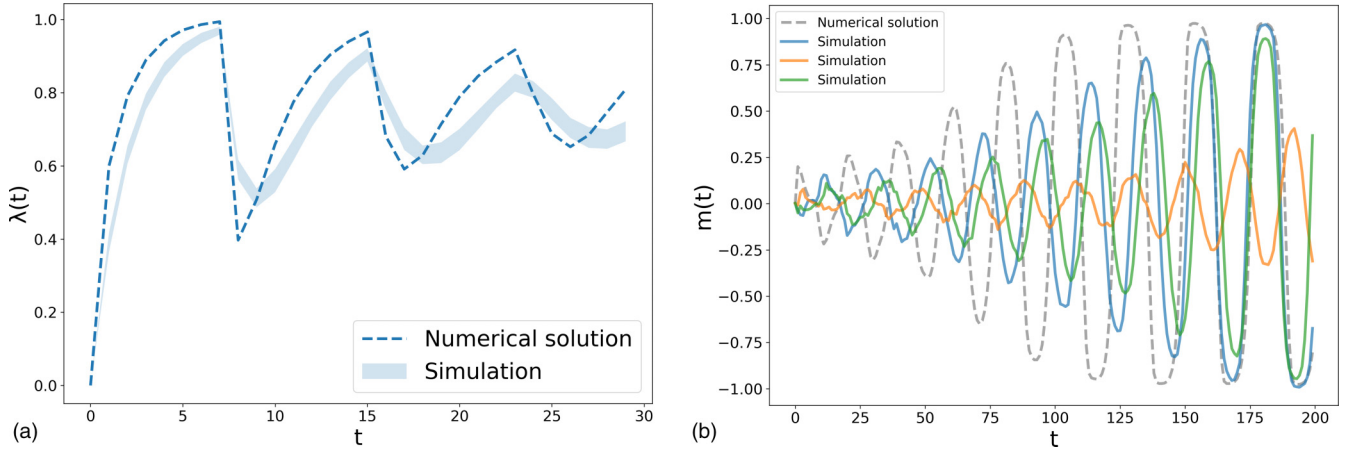


FIG. 3. Numerical solution compared to simulation runs of the model, for $l = 7$ and $N = 1000$. (a) Fraction of agents in the latency state. The dashed line is the solution of Eq. (6), whereas the solid band represents simulation results (confidence interval of 2 standard deviations for 100 runs of the model). (b) Magnetization of the system. The dashed line is the numerical solution of Eq. (5), while the solid curves represent different runs—which oscillate with the same period but have different phase and amplitude growth rates.

agent whatever her latency state) with a spin equal to ± 1 . Overall, we then have

$$\begin{aligned} \phi_{\mp\pm}(t) &= [1 - \lambda(t)] \left[\frac{N_{\mp}(t) - L_{\mp}(t)}{N - L(t)} \right] \left[\frac{N_{\pm}(t)}{N} \right] \\ &= \frac{1 \pm m(t)}{2} \left(\frac{1 \mp m(t)}{2} - \lambda_{\mp}(t) \right). \end{aligned} \quad (4)$$

We can now substitute such expressions into the expected values of m and λ_{\pm} , obtaining integral equations whose time derivative leads to the final system of differential equations describing the evolution of the VML:

$$m'(t) = 2 \left[\frac{1 - m(t)}{2} \lambda_{+}(t) - \frac{1 + m(t)}{2} \lambda_{-}(t) \right], \quad (5)$$

$$\begin{aligned} \lambda'_{\pm}(t) &= \left(\frac{1 \mp m(t)}{2} \right) \left[\frac{1 \pm m(t)}{2} - \lambda_{\mp}(t) \right] \\ &\quad - \left(\frac{1 \mp m(t-l)}{2} \right) \left[\frac{1 \pm m(t-l)}{2} - \lambda_{\mp}(t-l) \right]. \end{aligned} \quad (6)$$

The system above is a set of delay differential equations (DDEs with constant delay, which cannot be solved analytically due to their nonlinearity [36] (see Appendix C for an approximate solution for small values of m).

B. Numerical solution

As the evolution of $m(t)$ and $\lambda(t)$ ultimately depends only on the flip probabilities $\phi_{\mp\pm}(t)$, we tackle the system of DDEs (5) and (6) using the following iterative method. Starting from $\lambda(0) = 0$ and $m(0) = 10^{-6}$, at each time step t we (i) compute $\phi_{\mp\pm}$ as a function of m and λ_{\pm} , using Eq. (4); (ii) assess the number of flips as $N \phi_{\mp\pm}$, since N updates occur in a time step; and (iii) update m and λ_{\pm} according to Eqs. (5) and (6), then increase t . These steps are iterated until consensus or manual stop.

The proposed algorithm mimics model simulations and allows obtaining a numerical solution for the expected values

of $m(t)$ and $\lambda_{\pm}(t)$. Since the model dynamics is characterized by a deterministic drift, this approach works well in reproducing the peculiar oscillating behavior of $\lambda(t)$ [see Fig. 3(a)]. Additionally, we are able to control for finite-size effects, since the minimum increment is $2/N$ for m and $1/N$ for λ_{\pm} , which corresponds to the smallest distance the magnetization can reach from the full consensus state $|m| = 1$.

However, stochastic diffusion leads to randomness and thus plays an important role in determining the evolution of individual realizations of the VML. Indeed, while the period of the oscillations depends on the value of the latency time (see below), fluctuations set the growth rate of the amplitude and the phase of $m(t)$ [see Fig. 3(b)]. Therefore it is not straightforward to compare the evolution of simulations with the expected value of $m(t)$ from Eq. (5).

C. Dynamical origin of the oscillations

To explain why the VML shows an oscillating behavior, we focus on the flip probabilities of Eq. (4). In the initial configuration with $m = 0$ and no latent agents, the probabilities of having a flip to $+1$ or to -1 are equal. Random fluctuations then drive the evolution of the system. Suppose that at the first update the selected agent flips from -1 to $+1$. This means m increases by $2/N$ and λ_{+} by $1/N$, while λ_{-} is unchanged. As a result, ϕ_{+-} decreases with respect to ϕ_{-+} , and we have $\Delta\phi = \phi_{-+} - \phi_{+-} \simeq 1/(2N)$. Hence, at the next update, the magnetization is more likely to increase than to go back to zero, λ_{+} grows, and $\Delta\phi$ increases as well. This mechanism determines a drift that does not exist in the original voter model, where the two flip probabilities are always equal.

By iterating the above reasoning, we see that the agents in latency tend to have spin $+1$ (or more generally, the same spin as the sign of the magnetization). However, after l time steps, the agents that exit latency determine a decrease of λ_{+} (higher than that of λ_{-}) and a gradual reequilibration of the flip probabilities. Since these agents are not frozen anymore and so can change opinion to -1 , the growth of m slows down. Once some of them flip, λ_{-} starts growing and ϕ_{+-} becomes

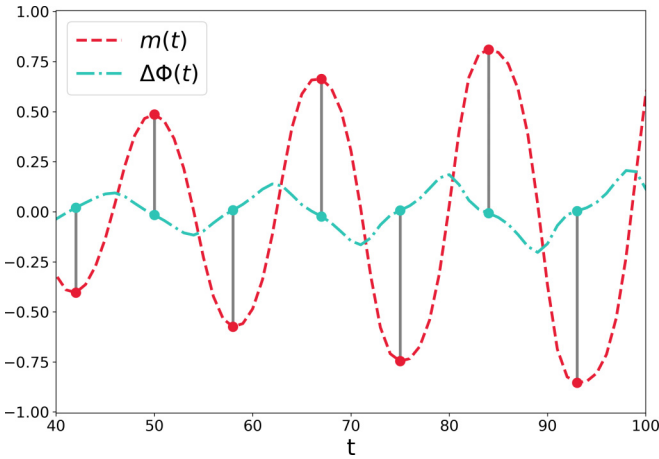


FIG. 4. (a) The numerical solution of $m(t)$ and $\Delta\phi(t)$ (here with $l = 5$) shows that these quantities oscillate with a quarter-period shift (markers on peaks of m correspond to zeros of $\Delta\phi$).

larger than ϕ_{-+} (i.e., $\Delta\phi$ becomes negative). We thus have the same situation just described but reverted towards the opposite sign of m . Opinion waves are hence due to agents with the same spin going into and exiting latency together.

Such a picture is confirmed by Fig. 4, where we plot the numerical solutions for $\Delta\phi(t)$ and $m(t)$ at steady state (i.e., far from the initial fluctuations); these quantities oscillate with a quarter-period shift.

D. Shape of the oscillations and asymptotic behavior

We finally investigate how the population size N and the latency time l influence the dynamics of the VML. First, we characterize the period and amplitude of the oscillations of $m(t)$. Figure 5 shows the period of the oscillations as a function of latency. The plot is limited to the region of l where oscillations are actually observed ($l \geq 3$) and no consensus is

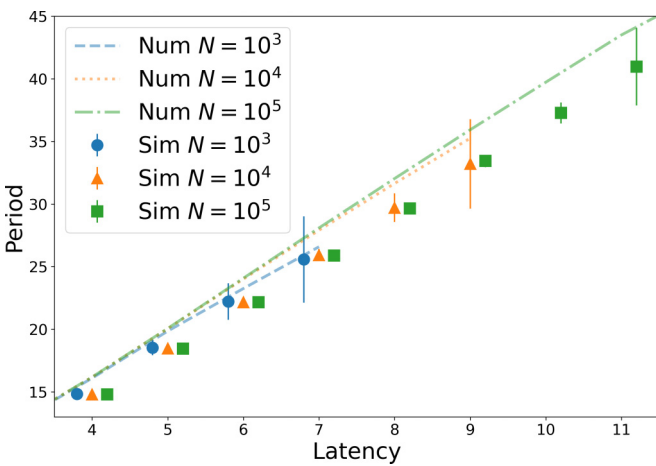


FIG. 5. Period of $m(t)$ (computed as the average distance between peaks over 100 runs per point) as a function of l , for both numerical solution and simulations. Markers are shifted to be readable despite the overlap, error bars represent 2 standard deviations. For each N we plot the values of l where the system does not reach consensus.

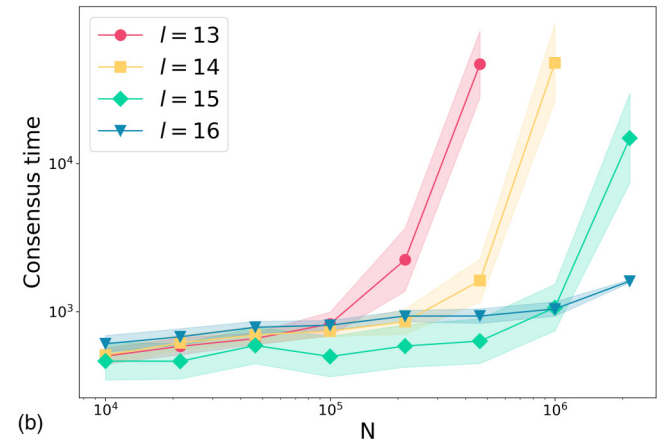
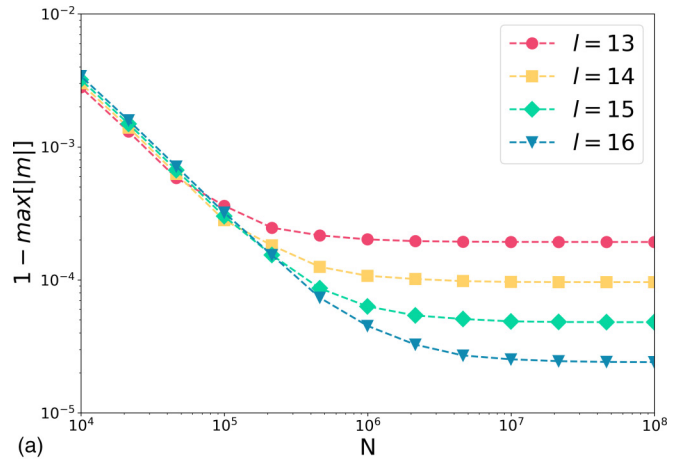


FIG. 6. (a) Minimum distance from the consensus state, $1 - \max_{s \leq t} |m(s)|$, achieved by the numerical solution as a function of the population size N . (b) Time to reach consensus in simulations as a function of N (averaged over 100 runs).

reached ($l \leq l_c$, a value that depends on N —see Appendix D). The period grows almost linearly as a function of l , and the agreement between simulations and the numerical solution is good, with simulations having slightly smaller period than the numerical solution.

Then we investigate whether the model dynamics is able to reach the consensus state. Figure 6 shows that the numerical solution never reaches $|m| = 1$; in the thermodynamic limit, opinions keep swinging forever. For large enough N , the amplitude of the oscillations stabilizes around a value that is smaller than 1 and independent of N . Note that the local maxima of m can be arbitrarily close to 1 but are always compatible with Eqs. (5) and (6) (see Appendix E). Importantly, for fixed N , longer latencies lead to higher oscillation amplitudes. This facilitates the reach of consensus in simulations for large values of l , as a finite-size effect. Indeed, as Fig. 6 shows, after a transient for small N , the time to reach consensus in simulations grows more than exponentially with the population size. For fixed N , longer latencies l are characterized by oscillations of higher amplitude and thus can reach the absorbing consensus state more easily due to stochastic fluctuations.

III. CONCLUSIONS

In this work we have shown how the addition of a simple ingredient in the voter model, namely, a constant latency time for agents after they change opinion, leads to the spontaneous emergence of deterministic dynamical oscillations in the average opinion. This behavior is totally different in nature both from the diffusive route to consensus of the original model and from the mean-reverting dynamics of noisy models that keep the system in a disordered state.

A key to obtain oscillations in the VML is the same latency time for each agent. Indeed, the higher the variability of individual latencies the weaker the oscillations (see Appendix F); when latency times are completely random, we recover the setup by Lambiotte *et al.* [23], characterized by a noisy evolution with no magnetization. The use of a common latency time for agents is however justified in contexts like political elections, particularly in the U.S., where they take place every four years and the voting population is almost equally split into two opinions only.

We note that an oscillatory pattern of the magnetization has been previously reported in the model with continuous aging by Pérez *et al.* [20], in the case where agents that have recently changed their opinion tend to impose their opinion on others. This mechanism thus differs substantially from that of the VML, where oscillations arise due to latency—that is, agents' reluctance to change newly acquired opinions.

The model can be generalized in many directions, for instance, using different interaction structures of the population, including more than two opinion states, or different rules for the latency state. For instance, if we consider the alternative dynamic rule whereby agents who maintain their opinion enter latency (rather than those who change it), we get a model formulation in which the route to consensus is accelerated by a deterministic drift (see Appendix G).

Overall, the preference for recently acquired opinions stands as a possible mechanism to consider for explaining social contexts characterized by opinion waves, alongside sociological factors such as government policy inertia [37] or psychological biases [38]. The proposed framework can thus find many applications within the broad universality class of the voter model [39].

APPENDIX A: ELECTORAL RESULTS FOR ALL US STATES

In the main text, we reported the case of 5 swing states to show their oscillating behavior. Actually, the elections in all the states show an oscillating pattern, as can be inferred by Fig. 7.

APPENDIX B: DETAILS ON NUMERICAL SIMULATIONS

To perform a simulation run of the model, we start by placing the N agents on the nodes of a fully connected graph, assigning each of them a spin $s_i \in \{\pm 1\}$ (with equal probability). Initially, no agent is in the latency state. Then we set the values of the parameters l (latency time) and t_{\max} (maximum length of the simulation). Starting from $t = 0$, at each step of the simulation (i) we randomly choose one target agent and one of its neighbors for the update; (ii) if the target agent is not

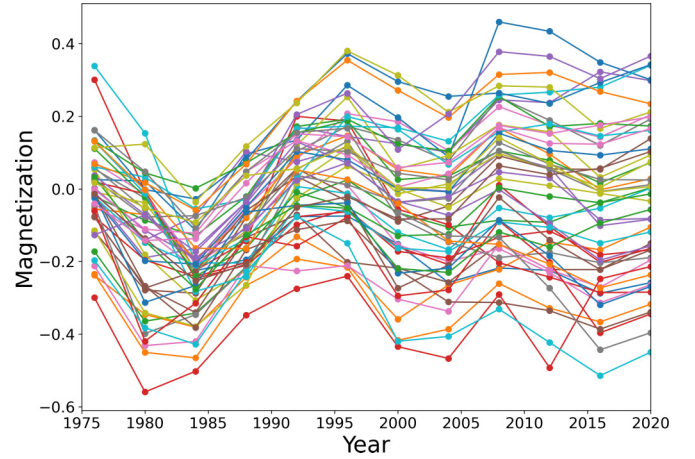


FIG. 7. Oscillations in elections results for all U.S. states (except DC). +1 represents a vote for Democrats and -1 for Republicans (votes for third parties are discarded, as they usually constitute less than 5% of the total votes). The so-called *swing states* are those that oscillate around $m = 0$ (and so they are crucial in determining the global outcome), yet all states in fact swing, following a common trend.

in latency and has a different spin than its chosen neighbor, the target agent flips (in all other cases, nothing happens); (iii) if the flip occurs, the target agent is put in latency for the next l time steps; and (iv) these steps are repeated until all agents have the same spin or $t = t_{\max}$.

APPENDIX C: APPROXIMATE SOLUTION FOR SMALL MAGNETIZATION

We can analyze the behavior of the system of DDEs, describing the expected values of $m(t)$ and $\lambda(t)$ [Eqs. (5) and (6)], for small values of m . This approximation leads to linear DDEs that can be solved with the step method. When $m = 0$, Eq. (6) becomes $\lambda'(t) = 1 - [\lambda(t) - \lambda(t-l)]/2$, whose solution for $t < nl$ with $n \in \mathbb{N}$ reads

$$\lambda(t) = 1 - \sum_{k=0}^{n-1} \frac{1}{k!} \left(\frac{t-kl}{2} \right)^k e^{-\frac{t-kl}{2}}. \quad (\text{C1})$$

As shown in Fig. 8, this solution works well in predicting the actual evolution of the system as soon as the magnetization maintains a value around 0, which is true for a significant amount of time. More importantly, it works as a proof of concept to understand the features and behavior of typical DDE solutions. As common in these cases, the function obtained is not a smooth \mathbb{C}^∞ function but a piecewise one, as evident from Eq. (C1). Indeed each term of the sum turns on until the n th one, where $t < nl$. The curve plotted in Fig. 8 has $n = 4$ and therefore corresponds to the approximate solution (for $3l < t < 4l$):

$$\lambda(t) = 1 - e^{-\frac{t}{2}} - \frac{1}{2} \left(\frac{t-2l}{2} \right)^2 e^{-\frac{t-2l}{2}} - \frac{1}{4} \left(\frac{t-3l}{3} \right)^3 e^{-\frac{t-3l}{3}}. \quad (\text{C2})$$

The typical solutions of DDEs are subject to smoothing [36]. It can in fact be proven that Eq. (C1) has a discontinuity of its

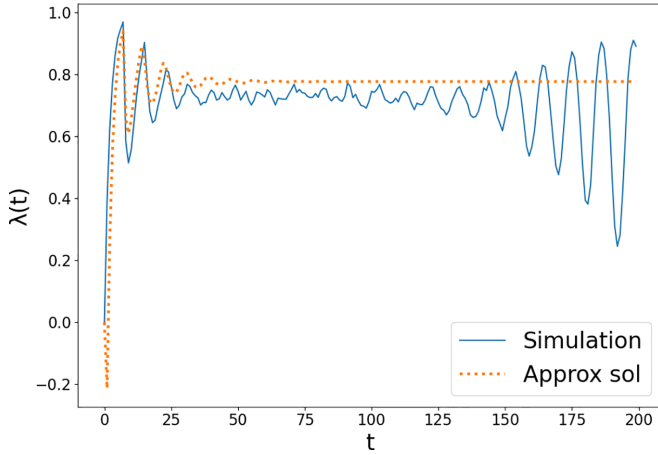


FIG. 8. The simulation and approximate solution [Eq. (C2)] for $\lambda(t)$ have good overlap for a large amount of time.

first derivative at $t = l$, a discontinuity of the second derivative at $t = 2l$, of the third at $t = 3l$, and so on, which makes the function smoother and smoother as time increases. Moreover, it can be easily proved that Eq. (C1) has a limit smaller than 1 for $t \rightarrow +\infty$, since (being all the terms positive)

$$1 - e^{-\frac{t}{2}} - \frac{1}{2} \left(\frac{t-2l}{2} \right)^2 e^{-\frac{t-2l}{2}} - \dots < 1 - e^{-\frac{t}{2}}, \quad (\text{C3})$$

and the right side of the equation asymptotically reaches 1. Yet this solution works well in predicting the actual value of λ only for a short time. When the oscillations of m reach a large amplitude, λ begins oscillating as well, as shown in Fig. 8.

APPENDIX D: MEASUREMENTS OF THE PERIOD

To detect the period of the oscillations of the main frequency of $m(t)$, we used the average distance between peaks. The period reaches its stationary value after a transient region, which lasts much longer in simulations than in the numerical solution (see Fig. 9). We sample after the transient to obtain

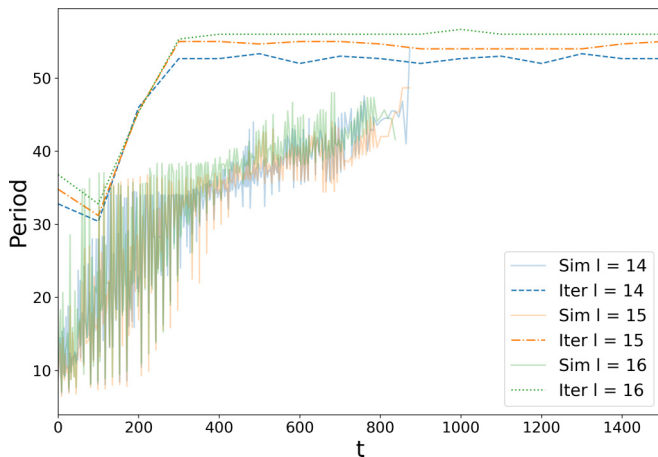


FIG. 9. Period of the oscillations for simulations and numerical solutions ($N = 10\,000$), computed on a moving time window of width 100. In these cases, simulations reach consensus before the period reaches a steady value.

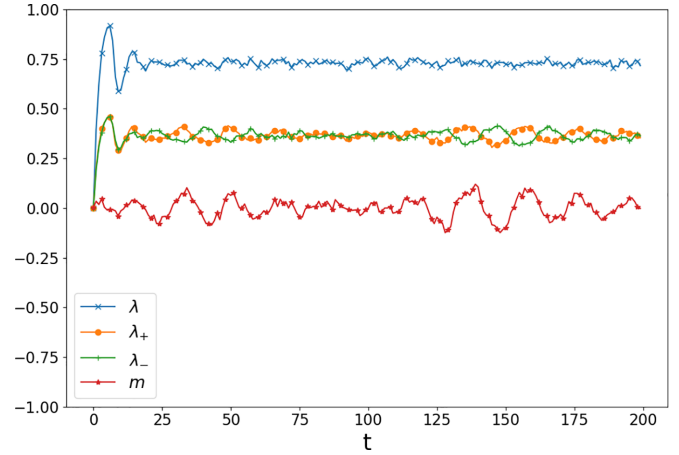


FIG. 10. Simulation with same parameters used in Fig. 2(a) but with agents having heterogeneous latency times.

reliable measurements (those reported in Fig. 5); however, for $l \gtrsim 10$ the period is not able to reach a stable value before consensus is reached due to random fluctuations, compromising its detection. Therefore we report only results until the region $l \gtrsim 10$ for $N = 10\,000$.

APPENDIX E: EXISTENCE OF LOCAL MAXIMA OF THE MAGNETIZATION SMALLER THAN 1

In the main text we provide evidence that the model dynamics can reach the consensus state only as a finite-size effect. Here we show that the model admits local maxima of m that are arbitrarily close to consensus. To this end we rewrite our equations in terms of $\Delta\lambda(t) = \lambda_+(t) - \lambda_-(t)$. We then get

$$m'(t) = \lambda(t) \left[\frac{\Delta\lambda(t)}{\lambda(t)} - m(t) \right]. \quad (\text{E1})$$

The stationary points of m are thus defined by $m = \Delta\lambda/\lambda$,⁵ a condition that can be rewritten as

$$m(t) = 1 - \frac{2\lambda_-(t)}{\lambda(t)}. \quad (\text{E2})$$

As m grows towards +1, λ_- also decreases so that m eventually reaches a value satisfying Eq. (E2) and smaller than 1. This is not an inflection point because m' changes sign there. We can conclude that the solutions of the model equations are compatible with the existence of local maxima at an arbitrarily small distance from 1. The same argument, of course, applies to the opposite case, $m = -1$.

APPENDIX F: HETEROGENEOUS LATENCY TIMES

Here we investigate what happens when the latency time is not the same for all agents. Figure 10 refers to the same configuration of Figs. 2(b), 3(a), and 3(b) but with agents having

⁵The fact that the solution of DDEs is not a \mathbb{C}^∞ function is not a limitation, because it only has a corner at $t = l$ and then gets smoother as time goes by. So we can rely on the condition on the first derivative to find the stationary points.

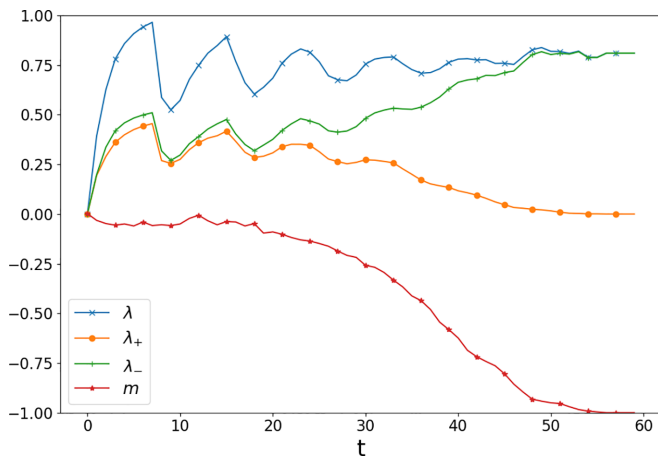


FIG. 11. Single run of the VML dynamics with opposite effect of latency [parameters $N = 1000$ and $l = 7$, the same setup used in Figs. 2(b), 3(a), and 3(b)].

heterogeneous latencies, distributed as a Gaussian centered at $\mu = 7$ with $\sigma = 1$. The dynamics become fuzzy, oscillations have higher frequencies, and the growth in amplitude changes

drastically. The broader the distribution of latencies the noisier the dynamics. For very heterogeneous latencies we retrieve the behavior observed in [23], where the magnetization remains around zero. This confirms that the swinging behavior emerges due to the synchronization of agents going into and exiting latency together.

APPENDIX G: OPPOSITE EFFECT OF LATENCY

Here we study an alternative model where agents go into latency when they are chosen for the update but do not flip. According to the discussion provided in Sec. II C, on the origin of oscillations in the VML, oscillations should not be present in this setup. Indeed, the evolution in the first l time steps is the same in the two versions of the model. Now at $t = l$, m has grown (say towards $+1$) and it is more likely to pick for the update an agent with $s = +1$. Since there are also more neighbors with $s = +1$, this agent is more likely to remain in her state than to flip, and so it goes into latency. Overall, agents with the same spin of the sign of m are likely to be in the latent state; they cannot change opinion and therefore the upward trend of m is locked and does not go back to 0. Thus in this opposite setup, latency gives rise to a drift that quickly pushes the system to the consensus state. This is confirmed by numerical simulations, reported in Fig. 11.

- [1] C. Castellano, S. Fortunato, and V. Loreto, *Rev. Mod. Phys.* **81**, 591 (2009).
- [2] S. Galam, *Sociophysics: A Physicist's Modeling of Psycho-Political Phenomena*, Understanding Complex Systems (Springer New York, New York, 2012).
- [3] S. Redner, *C. R. Phys.* **20**, 275 (2019).
- [4] A. F. Peralta, J. Kertész, and G. Iñiguez, Opinion dynamics in social networks: From models to data, [arXiv:2201.01322](https://arxiv.org/abs/2201.01322).
- [5] P. Clifford and A. Sudbury, *Biometrika* **60**, 581 (1973).
- [6] R. A. Holley and T. M. Liggett, *Ann. Probab.* **3**, 643 (1975).
- [7] T. C. Schelling, *J. Conflict Resolution* **17**, 381 (1973).
- [8] S. E. Asch, *Organizational Influence Processes* (Routledge, Milton Park, Abingdon, Oxfordshire, 2003), pp. 295–303.
- [9] S. Redner, *A Guide to First-Passage Processes* (Cambridge University Press, Cambridge, England, 2001).
- [10] P. Holme and F. Liljeros, *Front. Phys.* **3**, 78 (2015).
- [11] M. Galesic and D. L. Stein, *Physica A* **519**, 275 (2019).
- [12] A. C. R. Martins and S. Galam, *Phys. Rev. E* **87**, 042807 (2013).
- [13] S. Moscovici, in *Advances in Experimental Social Psychology* (Elsevier, New York, 1980), Vol. 13, pp. 209–239.
- [14] S. Moscovici, Innovation and minority influence, in *Perspectives on Minority Influence*, European Studies in Social Psychology, edited by E. v. Avermaet, G. Mugny, and S. Moscovici (Cambridge University Press, Cambridge, 1985), pp. 9–52.
- [15] M. Mobilia, A. Petersen, and S. Redner, *J. Stat. Mech.: Theory Exp.* (2007) P08029.
- [16] S. Galam and F. Jacobs, *Physica A* **381**, 366 (2007).
- [17] J. Xie, S. Sreenivasan, G. Korniss, W. Zhang, C. Lim, and B. K. Szymanski, *Phys. Rev. E* **84**, 011130 (2011).
- [18] H.-U. Stark, C. J. Tessone, and F. Schweitzer, *Phys. Rev. Lett.* **101**, 018701 (2008).
- [19] Z. Wang, Y. Liu, L. Wang, and Y. Zhang, *Sci. Rep.* **4**, 3597 (2014).
- [20] T. Pérez, K. Klemm, and V. M. Eguíluz, *Sci. Rep.* **6**, 21128 (2016).
- [21] A. F. Peralta, N. Khalil, and R. Toral, *Physica A* **552**, 122475 (2020).
- [22] J. W. Baron, A. F. Peralta, T. Galla, and R. Toral, *Entropy* **24**, 1331 (2022).
- [23] R. Lambiotte, J. Saramäki, and V. D. Blondel, *Phys. Rev. E* **79**, 046107 (2009).
- [24] R. Huo and R. Durrett, *Stoch. Proc. Appl.* **128**, 1590 (2018).
- [25] M. A. Montes de Oca, E. Ferrante, A. Scheidler, C. Pinciroli, M. Birattari, and M. Dorigo, *Swarm Intell.* **5**, 305 (2011).
- [26] A. Scheidler, *Phys. Rev. E* **83**, 031116 (2011).
- [27] M. E. Data and S. Lab, *Harvard Dataverse* (2017).
- [28] J. Fernández-Gracia, K. Suchecki, J. J. Ramasco, M. San Miguel, and V. M. Eguíluz, *Phys. Rev. Lett.* **112**, 158701 (2014).
- [29] D. Braha and M. A. M. de Aguiar, *PLOS ONE* **12**, e0177970 (2017).
- [30] A. Kononovicius, *Complexity* **2017**, 1 (2017).
- [31] S. Ansolabehere, J. Rodden, and J. M. Snyder, *J. Econ. Perspect.* **20**, 97 (2006).
- [32] W. G. Mayer, Public Perspective **3** (1992).
- [33] J. E. Roemer, Political cycles, *Econ. Politics* **7**, 1 (1995).
- [34] M. L. Atkinson, K. E. Coggins, J. A. Stimson, and F. R. Baumgartner, *The Dynamics of Public Opinion* (Cambridge University Press, Cambridge, 2021).

- [35] S. Gualdi, J.-P. Bouchaud, G. Cencetti, M. Tarzia, and F. Zamponi, *Phys. Rev. Lett.* **114**, 088701 (2015).
- [36] R. E. Bellman and K. L. Cooke, *Differential-Difference Equations* (Academic Press, Santa Monica, CA, 1963).
- [37] R. Soubeyran, *SSRN Electronic Journal* 10.2139/ssrn.912457 (2006).
- [38] E. Aragonès, *J. Theor. Politics* **9**, 189 (1997).
- [39] I. Dornic, H. Chaté, J. Chave, and H. Hinrichsen, *Phys. Rev. Lett.* **87**, 045701 (2001).